Using $X(3823) \to J/\psi\pi^+\pi^-$ to identify coupled-channel effects

Bo Wang[1,2],* Hao Xu[1,2],† Xiang Liu[1,2],‡ Dian-Yong Chen[1,2],§ Susana Coito[2],¶ and Estia Eichten[5]**

[1]*Research Center for Hadron and CSR Physics, Lanzhou University and Institute of Modern Physics of CAS, Lanzhou 730000, China*
[2]*School of Physical Science and Technology, Lanzhou University, Lanzhou 730000, China*
[3]*Research Center for Hadron and CSR Physics, Lanzhou University and Institute of Modern Physics of CAS, Lanzhou 730000, China*
[4]*Institute of Modern Physics, Chinese Academy of Sciences, Lanzhou 730000, China*
[5]*Theoretical Physics Department, Fermilab, IL 60510, USA*

Very recently, the Belle and BESIII experiments observed a new charmonium-like state $X(3823)$, which is a good candidate for the D-wave charmonium $\psi(1^3D_2)$. Because the $X(3823)$ is just near the $D\bar{D}^*$ threshold, the decay $X(3823) \to J/\psi\pi^+\pi^-$ can be a golden channel to test the significance of coupled-channel effects. In this work, this decay is considered including both the hidden-charm dipion and the usual quantum chromodynamics multipole expansion (QCDME) contributions. The partial decay width, the dipion invariant mass spectrum distribution $d\Gamma[X(3823) \to J/\psi\pi^+\pi^-]/dm_{\pi^+\pi^-}$, and the corresponding $d\Gamma[X(3823) \to J/\psi\pi^+\pi^-]/d\cos\theta$ distribution are computed. Many parameters are determined from existing experimental data, so the results depend mainly only on one unknown phase between the QCDME and hidden-charm dipion amplitudes.

PACS numbers: 14.40.Pq, 13.66.Bc
Keywords: Charmonium, Hidden-charm dipion decay

I. INTRODUCTION

Charmonium spectroscopy plays an important role in understanding strong interactions. New states appear continuously in experiments and are still puzzling, as they seem not to fit the model predictions. See Refs. [1–6] for reviews. However, some quark model low-lying states, such as the $\eta_{c2}(1^1D_2)$, $\psi(1^3D_2)$, or even the state $\psi(1^3D_3)$, are still missing [7]. Observation of the properties of these missing charmonium states can distinguish different phenomenological models, namely, quenched models, which consider only the naive $q\bar{q}$ spectrum (e.g., [8]), and unquenched models, where the coupled-channel effect is considered to be relevant [9].

Experiments show evidence of a state very likely to be interpreted as the $\psi(1^3D_2)$, the $X(3823)$. In 1994, the E705 experiment indicated a state in channel $J/\psi\pi^+\pi^-$ with 2.8σ and mass and width $m = 3836 \pm 13$ MeV and $\Gamma = 24 \pm 5$ MeV, respectively [10]. Interpretation as the 1^3D_2 was favored, since the 1^1D_2 decays into this channel is suppressed by G-parity, and the 1^3D_3 decays to the Okubo–Zweig–Iizuka (OZI)-allowed opened channel $D\bar{D}$, making it less likely to be seen in an OZI-suppressed channel. However, the observation of the $X(3823)$ was not confirmed by other experiments in the following 19 years. Finally, in 2013, Belle reported evidence of a new charmonium-like state in the radiative decay to $\chi_{c1}\gamma$ with mass $3823.1 \pm 1.8(\text{stat}) \pm 0.7(\text{syst})$ MeV and significance $3.8\,\sigma$ [11]. Very recently, BESIII confirmed the signal in the $\chi_{c1}\gamma$ invariant mass spectrum with a significance of 6.2σ in the process $e^+e^- \to \pi^+\pi^-\gamma\chi_{c1}$, with a measured mass of $3821.7 \pm 1.3(\text{stat}) \pm 0.7(\text{syst})$ MeV and a width of less than 16 MeV [12]. Therefore, the $X(3823)$ is now firmly established.

The $X(3823)$ is consistent with the theoretical prediction of the long-missing charmonium $\psi(1^3D_2)$ [13]. Although the mass of $\psi(1^3D_2)$ exceeds the $D\bar{D}$ threshold, the $\psi(1^3D_2) \to D\bar{D}$ channel is forbidden by parity conservation. Thus, no OZI-allowed open-charm decay modes exist, so the $\psi(1^3D_2)$ is expected to be a very narrow state. As a triplet state, the $\psi(1^3D_2)$ should typically decay to the $1^3S_1\pi\pi$, alias $J/\psi\pi\pi$, and decay radiatively to $1^3P_1\gamma$ and $1^3P_2\gamma$, alias $\chi_{c1}\gamma$ and $\chi_{c2}\gamma$, respectively. All of these channels have been analyzed in the above experiments, and enhancements have been detected. In addition, the upper limit for the ratio $B(X(3823) \to \chi_{c2}\gamma)/B(X(3823) \to \chi_{c1}\gamma)$ was given as < 0.41 by Belle and < 0.42 by BESIII; these values are consistent with prior theoretical calculations in Refs. [13–16], which give an upper ratio of around 0.24. In the same works, the partial decay width for $\psi(1^3D_2) \to J/\psi\pi^+\pi^-$ is estimated to be around 45 keV, a value well below the upper limit for the signal observed at E705. All this evidence strongly supports the identification of the $X(3823)$ with the $\psi(1^3D_2)$.

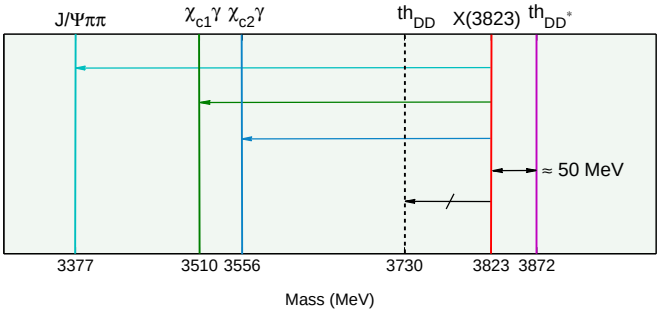

FIG. 1: (color online). Comparison of the mass of $X(3823)$ with the $D\bar{D}$ and $D\bar{D}^*$ thresholds, and some allowed and forbidden decay channels.

In theory, all OZI-allowed decay channels, which are not

*Electronic address: wangb13@lzu.edu.cn
†Electronic address: xuh2013@lzu.cn
‡Electronic address: xiangliu@lzu.edu.cn
§Electronic address: chendy@impcas.ac.cn
¶Electronic address: susana@impcas.ac.cn
**Electronic address: eichten@fnal.gov

forbidden by conservation of quantum numbers, have nonzero coupling to the bare state $q\bar{q}$ even if they are closed. We observe that the $D\bar{D}^*$ threshold lies only about 50 MeV above the mass of the $X(3823)$, as shown in Fig. 1. We suppose that the influence of $D\bar{D}^*$ in the $X(3823)$ state may be visible in its strong decay to $J/\psi\pi\pi$. This idea is supported by several studies of hadronic transitions between heavy quarkonia, suggesting the relevance of coupled-channel effects [17–23].

In the present work, the $X(3823)$ is assumed to be the $\psi(1^3D_2)$; inspired by the observation of the $X(3823)$ so near the $D\bar{D}^*$ threshold, we investigate the influence of the $D\bar{D}^*$ channel in the hidden-charm dipion decay $X(3823) \to J/\psi\pi^+\pi^-$. For this purpose, we study the dipion invariant mass and the scattering angle distributions of this process with and without the influence of $D\bar{D}^*$. Moreover, we try to compare the results with the sparse data from the E705 experiment. We employ two different methods. First, we apply the quantum chromodynamics multipole expansion (QCDME) [24] to study the decay $X(3823) \to J/\psi\pi^+\pi^-$ without the coupled-channel effects and obtain the distribution of the dipion invariant mass. Second, we calculate the same process including the hadronic loop mechanism, which is an effective description of the coupled-channel effect [18]. By adding $D\bar{D}^*$, we illustrate the change in the distributions of the dipion invariant mass and the polar angle with the interference of the coupled channel. Because these results might be accessible in current experiments, we consider that $X(3823) \to J/\psi\pi^+\pi^-$ is a golden channel to test the coupled-channel effect, and we also expect to motivate further analysis. We would like to note the relevance of this study to future theoretical development. The $\psi(1^3D_2)$ is a charmonium state, i.e., a heavy quark state, below all possible OZI-allowed thresholds. If we can show that coupling to a not-so-nearby closed channel is relevant to a faithful description of the state, this means that we surely cannot neglect the influence of the OZI-allowed decay channels in any serious description of resonances or light-quark systems [25].

This paper is organized as follows. In Sec. II, we describe the study of $X(3823) \to J/\psi\pi^+\pi^-$ via the QCDME method. In Sec. III, we present the calculation details of the same process using the hadronic loop mechanism, and in Sec. IV, we show numerical results for the dipion invariant mass and scattering angle including the coupled-channel effects. The paper ends with a summary in Sec. V.

II. STUDY OF $X(3823) \to J/\psi\pi^+\pi^-$ WITHOUT COUPLED-CHANNEL EFFECTS

In this section, we employ the QCDME method to study the hadronic transition $X(3823) \to J/\psi\pi^+\pi^-$ without considering any coupled-channel effect. The method has typically been applied to OZI-suppressed decays of heavy quarkonia with emission of light quarks and has proved to be reliable for general predictions of $\pi\pi$ invariant mass distributions and decay widths. The general idea is that a heavy quarkonium de-excites to a lower energy level, i.e., a lower radial level or orbital angular momentum level, by radiating gluons, in a manner very similar to that of the electromagnetic transitions within an atom. However, in contrast to the electromagnetic case, two complex vertices are involved; in the first vertex, we have multipole gluon emissions, whereas in the second vertex, hadronization occurs. Details of the QCDME method can be found in Refs. [17, 26, 27].

Our process is a transition between two triplet states, $1^3D_2 \to 1^3S_1\pi\pi$, which is dominated by double color-electric dipole emissions (E1-E1). By identifying Φ_i, Φ_f, and h with the initial and final heavy quarkonium $Q\bar{Q}$ states and the emitted light hadrons, respectively, the transition amplitude can be expressed as [17, 26]

$$\mathcal{M}_{E1-E1} = i\frac{g_E^2}{6}\left\langle \Phi_f h \left| \vec{x}\cdot\vec{E}G(E_i)\vec{x}\cdot\vec{E}\right| \Phi_i\right\rangle, \tag{1}$$

where g_E is the effective coupling constant for the chromoelectric multipole gluon emissions, $\vec{x}$ is the separation between Q and $\bar{Q}$, and $\vec{E}$ is the color-electric field. The Green function $G(E_i)$, where E_i is the initial state energy, is given by

$$G(E_i) = 1/(E_i - H_8 - iD_0) \tag{2}$$

with the gauge covariant time derivative

$$D_0 = \partial_0 - g\bar{A}_0. \tag{3}$$

Equations (2) and (3) represent propagation of the intermediate states between the two color-electric dipole vertices. In these vertices, we have color-singlet states composed of the $Q\bar{Q}$ color octet, gluons, and light quarks. The gluon field is represented by $\bar{A}_0$, and H_8 denotes the octet component of the Hamiltonian.

Equation (1) must be simplified to a calculable form. Because we do not understand the confinement mechanism, we need to introduce two further models to account for the unknown variables at both vertices. For the first vertex, we assume the quark-confining string model. Here, the intermediate states, i.e., those after emission of the first gluon g and before emission of the second gluon, are considered to be hybrid states. The ground state is simply a string between Q and $\bar{Q}$, and the first vibrational mode is the hybrid $Q\bar{Q}g$, the only one we keep. For the hadronization vertex, the soft-pion theorem is assumed.

After manipulating Eq. (1), we find that the transition rate $\Gamma(\Phi_i \to \Phi_f\pi\pi)$ between spin triplets with $l_i = 2$ and $l_f = 0$, where $l_{i,f}$ is the orbital momentum of the initial and final states, respectively, gives [27]

$$\Gamma[^3D \to {}^3S\pi^+\pi^-] = \frac{4}{15}\mathcal{H}\,|c_2|^2\,|f_{if}^1|^2, \tag{4}$$

where $\mathcal{H}$ denotes the phase-space integral:

$$\mathcal{H} = \frac{\pi^3 m_{J/\psi}}{20 m_X}\int dm_{\pi\pi}^2 \mathcal{K}\left(1-\frac{4m_\pi^2}{m_{\pi\pi}^2}\right)^{1/2}\left[\left(m_{\pi\pi}^2-4m_\pi^2\right)^2 \times\left(1+\frac{2}{3}\frac{\mathcal{K}^2}{m_{\pi\pi}^2}\right)+\frac{8\mathcal{K}^4}{15m_{\pi\pi}^4}\left(m_{\pi\pi}^4+2m_\pi^2m_{\pi\pi}^2+6m_\pi^4\right)\right], \tag{5}$$

where

$$\mathcal{K} = \frac{1}{2m_X}\Big[(m_X + m_{J/\psi})^2 - m_{\pi\pi}^2\Big]^{1/2}\Big[(m_X - m_{J/\psi})^2 - m_{\pi\pi}^2\Big]^{1/2}. \quad (6)$$

The dynamical part f_{if}^1 is expressed as

$$f_{if}^1 = \sum_n \frac{1}{m_i - m_{n1}}\left[\int dr r^3 \mathcal{R}_f(r)\mathcal{R}_{n1}(r)\right] \times\left[\int dr' r'^3 \mathcal{R}_{n1}(r')\mathcal{R}_i(r')\right], \quad (7)$$

where $\mathcal{R}_i(r)$, $\mathcal{R}_f(r)$, and $\mathcal{R}_{n1}(r)$ are the radial wave functions of the initial, final, and intermediate vibrational states, respectively, and the subscripts 1 and n correspond to the orbital angular momentum and radial quantum number, respectively. The radial wave functions are obtained numerically by solving the Schrödinger equation using the Cornell potential, which is defined as

$$V(r) = \frac{r}{a^2} - \frac{\kappa}{r}, \quad (8)$$

where $a = 2.34\ \text{GeV}^{-1}$ and $\kappa = 0.52$, and the constituent charm quark mass m_c is 1.84 GeV [27].

To obtain the radial wave function R_{n1} of the intermediate vibrational states, we introduce the potential model given in Ref. [28]:

$$V_\nu(r) = V(r) + \left[V_n(r) - \frac{1}{a^2}r\right] + \frac{A_\nu}{r}. \quad (9)$$

Here, $V(r)$ is listed in Eq. (8), and $V_n(r)$ is given by

$$V_n(r) = \frac{1}{a^2}r\left[1 + \frac{2\pi a^2 n}{(r-2d)^2 + 4d^2}\right]^{1/2} \equiv \frac{1}{a^2}r[2 - \alpha_n^2(r)]^{-1/2},$$
$$d = \frac{r^2\alpha_n(r)}{4a^2[2m_c + (1/a^2)r\alpha_n(r)]}. \quad (10)$$

We consider only the lowest string excitation, which corresponds to $n = 1$ in Eq. (10), and adjust the constant A_ν to fit the mass of the lowest vibrational state. As treated in Ref. [27], $m_\nu = 4.03$ GeV is taken as the mass of the ground state of the $c\bar{c}$ vibrational spectrum.

To determine the unknown parameter c_2 in Eq. (4), we use our knowledge of the decays $\psi(3686) \to J/\psi\pi^+\pi^-$ and $\psi(3770) \to J/\psi\pi^+\pi^-$, which are both transitions between triplet states. Here, we consider the mixing

$$\psi(3686) = \psi_{2S}\cos\theta + \psi_{1D}\sin\theta,$$
$$\psi(3770) = -\psi_{2S}\sin\theta + \psi_{1D}\cos\theta. \quad (11)$$

From the nonrelativistic formulas for the leptonic decay widths and the experimental values for the decays $\psi(3686), \psi(3770) \to e^+e^-$, the mixing angle is found to be around -10°. Moreover, the decay amplitude for $\psi(3686), \psi(3770)$ involves a mixture between Eq. (4) and a similar expression for the decay $\Gamma(^3S \to {}^3S\pi\pi)$, which involves a new parameter, c_1. However, as there are accurate data for the transitions $\psi(3686), \psi(3770) \to J/\psi\pi\pi$, both parameters, c_1 and c_2, are fully determined. We obtain $|c_2|^2 \simeq 1.46\times10^{-4}$ for the partial width in $\psi(^3D_2) \to J/\psi\pi^+\pi^-$.

For the process $X(3823) \to J/\psi\pi^+\pi^-$, Eqs. (5)–(8) give the results $\mathcal{H} = 0.0176\ \text{GeV}^7$ and $f_{if}^1 = -11.4\ \text{GeV}^{-3}$. Finally, the partial decay width becomes

$$\Gamma[X(3823) \to J/\psi\pi^+\pi^-] \simeq 89.1\ \text{keV}, \quad (12)$$

which is about two times larger than the previous result in Ref. [13].

We first consider the $\Gamma(X(3823) \to J/\psi\pi^+\pi^-)$ distribution over the $\pi^+\pi^-$ invariant mass, commonly called the dipion invariant mass distribution for simplicity. The result is shown in Fig. 2 (a). The lower $m_{\pi\pi}$ kinematic region is dominated by the S-wave contribution in the $\pi^+\pi^-$ propagation, whereas the peak around 0.65 GeV in the $\pi^+\pi^-$ invariant mass spectrum is due to the D-wave contribution [29]. We also show the corresponding experimental data from the E705 [10] experiment in Fig. 2 (b). A comparison of our QCDME results with the experimental data indicates a clear discrepancy in the $m_{\pi^+\pi^-}$ low-momentum region. This result is somewhat expected because more nonperturbative effects should be revealed at lower energies. Because QCDME appears to be insufficient to describe the data, we need to consider a new effect on $X(3823) \to J/\psi\pi^+\pi^-$. As mentioned in Sec. I, the proximity of $X(3823)$ to the closed $D\bar{D}^*$ threshold inspires our interest in studying the coupled-channel effects in the decay. This will be the task in the next section.

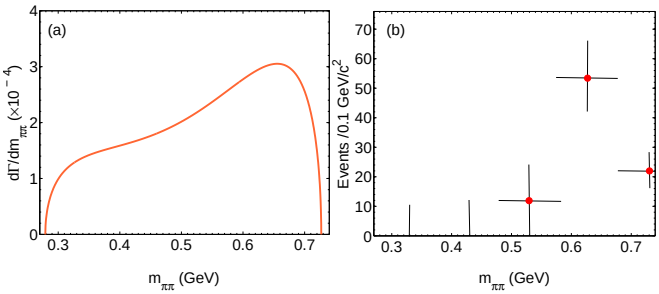

FIG. 2: (color online). The $\pi^+\pi^-$ invariant mass distribution $d\Gamma[X(3823) \to J/\psi\pi^+\pi^-]/dm_{\pi^+\pi^-}$ calculated using the QCDME method (left-hand panel) and the experimental data from E705 [10] (right-hand panel).

III. INCLUDING THE COUPLED-CHANNEL EFFECTS

In this section, we adopt the effective Lagrangian approach, which was previously used for several other quarkonium systems [30–33], to study the decay $X(3823) \to J/\psi\pi^+\pi^-$ by including hadronic loops, i.e., coupled-channel effects. Figure 3 shows diagrams illustrating the processes on the hadron level, where the triangle diagrams in (b) and (c) represent the

coupled-channel contribution. Here, the decay $X(3823) \to J/\psi\pi^+\pi^-$ occurs in two steps, $X(3823) \to D\bar{D}^* + h.c.$, followed by (b) $D\bar{D} \to \sigma \to \pi^+\pi^-$ or (c) $D^*\bar{D}^* \to \sigma \to \pi^+\pi^-$, and $D\bar{D}^* + h.c. \to J/\psi$.

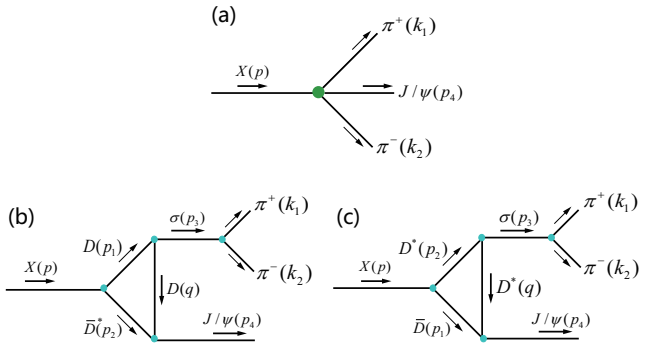

FIG. 3: (color online). Diagrams describing $X(3823) \to J/\psi\pi^+\pi^-$. Diagram (a) represents the direct decay process without considering the coupled-channel effects, whereas diagrams (b) and (c) show the coupled-channel contribution.

For the direct diagram in Fig. 3 (a), we adopt the method in Refs. [29, 34, 35], which are also based on the concepts of QCDME. The conversion of gluons into two pions is described by the matrix element $\langle\pi^+(k_1)\pi^-(k_2)|g^2F^a_{\mu\nu}(x)F^a_{\lambda\sigma}(x)|0\rangle$, where g is the QCD coupling constant, a is the color index, and $F^a_{\mu\nu}(x)$ is the gluon field strength operator. This matrix element can be uniquely determined using triangle anomalies and the trace of the energy-momentum tensor, as well as the soft pion approximation (see Refs. [34, 35] for more detailed derivations). Voloshin [29, 35] constructed the amplitude of the $\pi\pi$ transition between heavy quarkonium and explicitly separated the S- and D-wave contributions in the matrix element. For the direct diagram shown in Fig. 3 (a), the decay amplitude is [29, 35]

$$\mathcal{M}^{(a)} = ig_{XJ/\psi\pi\pi}\epsilon_{\kappa\lambda\nu\sigma}ip_4^\kappa\epsilon^{*\lambda}_{J/\psi}\epsilon^\nu_{X\mu}\left[\frac{2}{3}\left(1+\frac{2m_\pi^2}{p_3^2}\right)p_3^\sigma p_3^\mu - \ell^{\sigma\mu}\right] \quad (13)$$

with

$$\ell^{\sigma\mu} = \tilde{q}^\sigma\tilde{q}^\mu + \frac{1}{3}\left(1-4m_\pi^2/p_3^2\right)(p_3^2g^{\sigma\mu} - p_3^\sigma p_3^\mu), \quad (14)$$

where $g_{XJ/\psi\pi\pi}$ is the partial coupling constant corresponding to the direct process $X(3823) \to J/\psi\pi^+\pi^-$, $\epsilon_{\kappa\lambda\nu\sigma}$ is the antisymmetric symbol, and $\epsilon^{*\lambda}_{J/\psi}$ and $\epsilon^\nu_{X\mu}$ correspond to the polarization vector of J/ψ and polarization tensor of $X(3823)$, respectively. The first and second terms are defined as $p_3 = k_1 + k_2$ and $\tilde{q} = k_1 - k_2$, where k_1, k_2 corresponds to the $\pi^+\pi^-$ 4-momentum; these terms represent the S- and D-wave contributions to dipion propagation, respectively.

For the diagrams with hadron loops in Fig. 3 (b) and (c), we use the heavy quark effective model. For a heavy-light meson system, in the heavy quark limit $m_Q \to \infty$, there is heavy quark spin symmetry and heavy quark flavor symmetry. However, for a heavy quarkonium such as charmonium, heavy quark flavor symmetry will not hold while heavy quark spin symmetry still exists [36]. Thus, for charmonium systems, states with a given orbital angular momentum L but different spins form a multiplet. For example, the $L = 0$ (S-wave) charmonium spin doublet $\mathcal{J}$ can be written as [37, 38]

$$\mathcal{J} = \frac{1+\not{v}}{2}\left[J/\psi^\mu\gamma_\mu - \eta_c\gamma_5\right]\frac{1-\not{v}}{2}, \quad (15)$$

where v^μ is the 4-velocity of the multiplet, and J/ψ^μ and η_c are the spin-1 and spin-0 components, respectively. The general form of the orbital angular momentum $L \neq 0$ multiplet has been established in Refs. [36, 37]. For $L = 2$, the charmonium multiplet is given by

$$\begin{aligned}\mathcal{J}^{\mu\lambda} &= \frac{1+\not{v}}{2}\left[X_3^{\mu\lambda\alpha}\gamma_\alpha + \frac{1}{\sqrt{6}}\left(\epsilon^{\mu\alpha\beta\rho}v_\alpha\gamma_\beta X_\rho^\lambda + \epsilon^{\lambda\alpha\beta\rho}v_\alpha\gamma_\beta X_\rho^\mu\right)\right.\\ &+\frac{\sqrt{15}}{10}\left[(\gamma^\mu - v^\mu)\psi^\lambda + (\gamma^\lambda - v^\lambda)\psi^\mu\right]\\ &\left.-\frac{1}{\sqrt{15}}\left(g^{\mu\lambda} - v^\mu v^\lambda\right)\gamma_\alpha\psi^\alpha + \eta_2^{\mu\lambda}\gamma_5\right]\frac{1-\not{v}}{2}, \quad (16)\end{aligned}$$

where all the tensor fields are traceless, symmetric, and transverse. The fields X_3, X, ψ, and η_2 denote the charmonia with $J^{PC} = 3^{--}$, 2^{--}, 1^{--}, and 2^{-+}, respectively, where X and ψ correspond to $X(3823)$ and $\psi(3770)$, respectively.

The effective Lagrangian describing the open charm mesons interacting with the S- and D-wave charmonium multiplet is given by

$$\begin{aligned}\mathcal{L} &= g'\mathrm{Tr}\left[\mathcal{J}\bar{H}_2\overleftrightarrow{\partial}_\mu\gamma^\mu\bar{H}_1\right] + \mathrm{H.c.},\\ \mathcal{L} &= g\mathrm{Tr}\left[\mathcal{J}^{\mu\lambda}\bar{H}_2\overleftrightarrow{\partial}_\mu\gamma_\lambda\bar{H}_1\right] + \mathrm{H.c.}, \quad (17)\end{aligned}$$

where $\overleftrightarrow{\partial} = \overrightarrow{\partial} - \overleftarrow{\partial}$. The mesons with a single heavy quark are represented by $H_{1,2}$, which is defined as

$$H_1 = \frac{1+\not{v}}{2}\left[D^{*\mu}\gamma_\mu - D\gamma_5\right], \quad (18)$$

$$H_2 = \left[\bar{D}^{*\mu}\gamma_\mu - \bar{D}\gamma_5\right]\frac{1-\not{v}}{2}, \quad (19)$$

and form a doublet with $l = 0$, $J^P = (0^-, 1^-)$. The field $D^{(*)}$ includes a normalization factor $\sqrt{m_{D^{(*)}}}$, and $\bar{H}_{1,2} = \gamma^0 H^\dagger_{1,2}\gamma^0$.

Using Eqs. (16)–(19), we obtain an explicit expression for the Lagrangian density of $X(3823)$ and $\psi(3770)$ coupling to the charmed meson pair:

$$\mathcal{L}_{XDD^*} = ig_{XD^*D}X^{\mu\nu}\left[\bar{D}\overleftrightarrow{\partial}_\nu D^*_\mu - \bar{D}^*_\mu\overleftrightarrow{\partial}_\nu D\right], \quad (20)$$

$$\mathcal{L}_{\psi DD} = g_{\psi DD}\psi^\mu(\bar{D}\partial_\mu D - D\partial_\mu\bar{D}), \quad (21)$$

where

$$g_{XD^*D} = 2g\sqrt{\frac{3}{2}}\sqrt{m_X m_{D^*}m_D}, \quad (22)$$

$$g_{\psi DD} = -2g\frac{\sqrt{15}}{3}\sqrt{m_\psi}m_D. \quad (23)$$

For the vertices in Fig. 3 (b) and (c) involving J/ψ, we use Eqs. (15) and (17)-(19), which yield

$$\mathcal{L}_{J/\psi DD^*} = ig_{J/\psi DD^*}\epsilon_{\alpha\rho\beta\lambda}[\bar{D}\overleftrightarrow{\partial}^{\alpha}D^{*\rho} - \bar{D}^{*\rho}\overleftrightarrow{\partial}^{\alpha}D]\partial^{\beta}J/\psi^{\lambda}. \quad (24)$$

The effective Lagrangians for the other vertices are given by Refs. [30–33].

$$\mathcal{L}_{\sigma DD} = -g_{\sigma DD}D\bar{D}\sigma, \quad (25)$$
$$\mathcal{L}_{\sigma D^*D^*} = g_{\sigma D^*D^*}D^*\cdot\bar{D}^*\sigma, \quad (26)$$
$$\mathcal{L}_{\sigma\pi\pi} = g_{\sigma\pi\pi}\sigma\pi\pi. \quad (27)$$

Given the above Lagrangian densities, the decay amplitudes corresponding to the triangle diagrams in Fig. 3, with the p_i 4-momentum defined in the figure, are

$$\mathcal{M}^{(b)} + \mathcal{M}^{(c)} = \left[\mathcal{M}^{D}_{D\bar{D}^*} + \mathcal{M}^{D^*}_{\bar{D}D^*}\right] \times \frac{\sqrt{2}g_{\sigma\pi\pi}}{p_3^2 - m_\sigma^2 + im_\sigma\Gamma_\sigma}, \quad (28)$$

where

$$\begin{aligned}\mathcal{M}^{D}_{D\bar{D}^*} &= (i)^3\int\frac{d^4q}{(2\pi)^4}\Big[ig_{XDD^*}\epsilon^{\nu}_{X\mu}(ip_{2\nu} - ip_{1\nu})\Big]\Big[-g_{\sigma DD}\Big] \\ &\times\Big[ig_{J/\psi DD^*}\epsilon_{\alpha\rho\beta\lambda}(iq^{\alpha} - ip_2^{\alpha})ip_4^{\beta}\epsilon^{*\lambda}_{J/\psi}\Big]\frac{1}{p_1^2 - m_D^2} \\ &\times\frac{1}{q^2 - m_D^2}\frac{-g^{\mu\rho} + p_2^{\mu}p_2^{\rho}/m_{D^*}^2}{p_2^2 - m_{D^*}^2}\mathcal{F}^2(q^2), \end{aligned} \quad (29)$$

$$\begin{aligned}\mathcal{M}^{D^*}_{\bar{D}D^*} &= (i)^3\int\frac{d^4q}{(2\pi)^4}\Big[ig_{XDD^*}\epsilon^{\nu}_{X\mu}(ip_{2\nu} - ip_{1\nu})\Big]\Big[g_{\sigma D^*D^*}\Big] \\ &\times\Big[ig_{J/\psi DD^*}\epsilon_{\alpha\rho\beta\lambda}(-iq^{\alpha} + ip_1^{\alpha})ip_4^{\beta}\epsilon^{*\lambda}_{J/\psi}\Big]\frac{1}{p_1^2 - m_D^2} \\ &\times\frac{-g^{\mu\tau} + p_2^{\mu}p_2^{\tau}/m_{D^*}^2}{p_2^2 - m_{D^*}^2}\frac{-g^{\rho\tau} + q^{\rho}q^{\tau}/m_{D^*}^2}{q^2 - m_{D^*}^2}\mathcal{F}^2(q^2). \end{aligned} \quad (30)$$

In Eqs. (29) and (30), we introduce the monopole form factor

$$\mathcal{F}(q^2) = (m_E^2 - \Lambda^2)/(q^2 - \Lambda^2), \quad \Lambda = m_E + \alpha\Lambda_{QCD} \quad (31)$$

to account for the unknown structure and the significant off-shell effect of the exchanged $D^{(*)}$ mesons [18, 39], where m_E and q denote the mass and 4-momentum of the exchanged $D^{(*)}$ mesons, respectively, and $\Lambda_{QCD} = 220$ MeV. In Eq. (28), we adopt the momentum-dependent form of Γ_σ for the propagator of the σ meson [40] because the total decay width and mass are of the same order, i.e.,

$$\Gamma_\sigma(m_{\pi^+\pi^-}) = \Gamma_\sigma\frac{m_\sigma}{m_{\pi^+\pi^-}}\frac{|\vec{p}(m_{\pi^+\pi^-})|}{|\vec{p}(m_\sigma)|}, \quad (32)$$

where $|\vec{p}(m_{\pi^+\pi^-})| = \sqrt{m^2_{\pi^+\pi^-}/4 - m_\pi^2}$ is the pion momentum, and $|\vec{p}(m_\sigma)|$ is the pion momentum with an on-shell σ meson.

After the loop integrals in Eqs. (29) and (30) are performed, the decay amplitudes in Eq. (28) can be further parameterized as

$$\mathcal{M}^{(b)} + \mathcal{M}^{(c)} = 4\mathcal{A}p_{3\theta}p_{3\nu}p_{4\eta}\epsilon^{\lambda\mu\theta\eta} \times \frac{\sqrt{2}g_{\sigma\pi\pi}(\epsilon^{\nu}_{X\mu}\epsilon^{*}_{J/\psi\lambda})}{p_3^2 - m_\sigma^2 + im_\sigma\Gamma_\sigma}, \quad (33)$$

where the amplitudes can be contracted to one independent Lorentz structure, and all the factors are included in $\mathcal{A}$. The factor 4 comes from the contributions of four possible intermediate channels: $D^0\bar{D}^{*0}$, $\bar{D}^0D^{*0}$, D^+D^{*-}, and D^-D^{*+}. Further, $\sqrt{2}$ is the isospin factor of π^+ and π^-.

Finally, the total contribution to $X(3823) \to J/\psi\pi^+\pi^-$ from the three Feynman diagrams in Fig. 3 is

$$\mathcal{M}_{\rm Total} = \mathcal{M}^{(a)} + e^{i\Phi}[\mathcal{M}^{(b)} + \mathcal{M}^{(c)}], \quad (34)$$

where we introduce the phase angle Φ as a measure of the interference between the amplitudes of the triangle and direct diagrams. According to the three-body decay formula [7], the differential decay width for $X(3823) \to J/\psi\pi^+\pi^-$ is

$$d\Gamma = \frac{1}{(2\pi)^3}\frac{1}{32M_X^3}\overline{|\mathcal{M}_{\rm Total}|^2}dm^2_{J/\psi\pi^+}dm^2_{\pi^+\pi^-}, \quad (35)$$

where $m^2_{J/\psi\pi^+} = (p_4 + k_1)^2$, and $m^2_{\pi^+\pi^-} = (k_1 + k_2)^2$.

Before presenting our result, we need to determine the values of the coupling constants. The global coupling constant g appearing in Eq. (17) can be obtained from Eqs. (21) and (23) because we know the experimental value, $\Gamma[\psi(3770) \to D^0\bar{D}^0] = 14.1$ MeV [7]. The constant is thus $g = 1.37$ GeV$^{-3/2}$. From Eq. (22), we obtain the coupling constant $g_{XDD^*} = 12.7$. Additionally, the coupling constant $g_{J/\psi DD} = 8$ in Eq. (24) can be related to $g_{J/\psi DD^*}$, which is calculated using the vector meson dominance model and the QCD sum rule [41–43]. Under heavy quark symmetry, we have the relation $g_{J/\psi DD} = g_{J/\psi D^*D^*} = m_D g_{J/\psi DD^*}$. Furthermore, $g_{\sigma DD}$ and $g_{\sigma D^*D^*}$ satisfy $g_{\sigma DD} = g_{\sigma D^*D^*} = m_{D^*}g_\pi/\sqrt{6}$ with $g_\pi = 3.73$ [44, 45]. We use $m_\sigma = 526$ MeV for the the mass of the σ meson in our calculation. By fitting the decay width $\Gamma(\sigma \to \pi^+\pi^-) = 200$ MeV [46], we obtain the coupling constant $g_{\sigma\pi\pi} = 1.8$ GeV. These values are summarized in Table I.

With the above coupling constants as input, we first show the dependence on α, in Eq. (31), of the decay width of $X(3823) \to J/\psi\pi^+\pi^-$ if we consider only the contributions from Fig. 3 (b) and (c). The result, which is shown in Fig. 4, indicates that the contribution from the coupled-channel effect to $X(3823) \to J/\psi\pi^+\pi^-$ becomes larger when α is increased. At present, we cannot fix the value of α using the experimental data. We choose a typical value of $\alpha = 4.2$ as adopted in Ref. [33], where the decay width from the coupled-channel effect only is comparable with that from the direct decay.

IV. COUPLED-CHANNEL RESULTS

Now, we have fixed all the parameters in our work except for the phase angle Φ in Eq. (34). Without any exper-

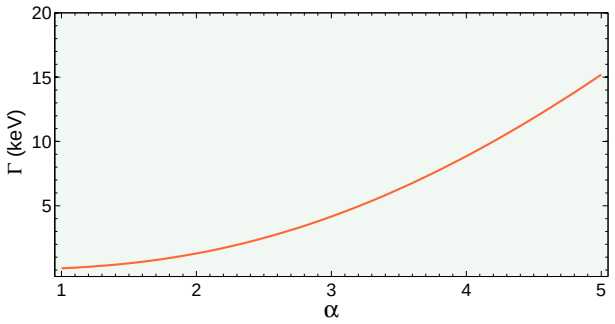

FIG. 4: (color online). Dependence of the decay width of $X(3823) \to DD^* \to J/\psi\pi^+\pi^-$ on α and phase angle Φ considering only Fig. 3 (b) and (c).

TABLE I: Values of the parameters used in our calculations.

$m_{X(3823)}$	$m_{J/\psi}$	m_D	m_{D^*}	m_π
3.823 GeV	3.096 GeV	1.865 GeV	2.007 GeV	0.139 GeV
$g_{XJ/\psi\pi\pi}$	g_{XDD^*}	$g_{\psi DD}$	$g_{J/\psi DD^*}$	$g_{J/\psi DD}$
12.4 GeV^{-1}	12.7	-12.8	4.3 GeV^{-1}	8
$g_{\sigma DD}$ ($g_{\sigma D^*D^*}$)	$g_{\sigma\pi\pi}$	m_σ	Γ_σ	α
3.1 GeV	1.8 GeV	0.526 GeV	0.302 GeV	4.2

imental constraints, this parameter is entirely free. Therefore, we compute the dependence of the total decay width of $X(3823) \to J/\psi\pi^+\pi^-$ on the phase angle Φ, the $\pi^+\pi^-$ invariant mass distribution $d\Gamma[X(3823) \to J/\psi\pi^+\pi^-]/dm_{\pi^+\pi^-}$, and the polar angle distribution $d\Gamma[X(3823) \to J/\psi\pi^+\pi^-]/d\cos\theta$ for Φ values ranging over the entire trigonometric circle. These results are presented in Fig. 5 and Fig. 6. The total decay width and the $\pi^+\pi^-$ invariant mass distribution are found to vary dramatically with Φ, but the polar angle distributions almost keep the fixed line-shape. For Φ within the third and fourth quadrants, the S-wave part is dominant, and most

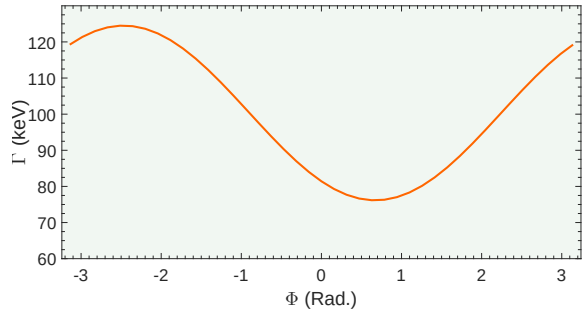

FIG. 5: (color online). Dependence of the total decay width of $X(3823) \to J/\psi\pi^+\pi^-$ on phase angle Φ considering Fig. 3 (a), (b), and (c). Here, α was fixed at 4.2 to obtain these results.

events scatter perpendicularly to the initial particle momentum, although the particular shape of the distribution changes slightly with the variation of Φ. However, when Φ lies in the first and second quadrant, the contribution from S-wave is largely suppressed and D-wave becomes the dominant one, the angular distribution stays the same with when Φ lies in the third and fourth quadrant. Except for the cases $\Phi = 3\pi/4$, it is difficult to distinguish which partial wave contribution is bigger in the $\pi^+\pi^-$ propagation, there seems to be a symmetric relation between the dominance of different partial wave and the value of Φ. Fig. 6 shows that we can't qualitatively judge the relative phase Φ from angle distribution, thus the precise measurement about the $\pi^+\pi^-$ mass spectrum is needed.

When we compare this result with the result from QCDME in Fig. 2 (a), we see there is always a difference between the $m_{\pi^+\pi^-}$ distributions with and without coupled-channel interference, for any angle Φ, although for small Φ angles, the results become more similar. In addition, when we compare the results in Fig. 6 with the sparse data in Fig. 2 (b), we see that small angles for Φ are favored. Finally, the full widths, also given in Fig. 6, are sensitive to Φ as well. Given the analysis, we conclude that only data, so far sparse or nonexistent for $X(3823) \to J/\psi\pi^+\pi^-$, can yield more definite conclusions.

V. SUMMARY AND CONCLUSIONS

Very recently, a true charmonium-like state, $X(3823)$, was established by the Belle and BESIII collaborations in the radiative decay channel $\chi_{c1}\gamma$. Moreover, a signal with low statistics was found two decades ago, by the E705 experiment in the same energy region, but in the hadronic decay channel $J/\psi\pi^+\pi^-$. This new state is most likely to be the missing charmonium $\psi(1^3D_2)$.

In this work, we studied the decay $X(3823) \to J/\psi\pi^+\pi^-$ within two different theoretical frameworks, the QCDME and the effective Lagrangian approach, including hadronic loops. The first method accounts for only the direct process, whereas the second method includes, not only the direct process, but also the coupled-channel effects due to the nearby closed OZI-allowed channel $D\bar{D}^*$. We computed the partial decay width distribution with the dipion invariant mass, $\Gamma[X(3823) \to J/\psi\pi^+\pi^-]/dm_{\pi^+\pi^-}$, within both approaches. If we neglect the coupled-channel effect and only consider the direct decay $X(3823) \to J/\psi\pi^+\pi^-$, within QCDME, we find disagreement with the scarce data from the E705 experiment, in particular for lower values of the dipion kinetic energy. This type of inaccuracy of the QCDME has been discussed in other works [17], as the method does not include nonperturbative effects. If we include the coupled-channel by using the hadronic loop mechanism, we see there is always interference between the direct process and the indirect processes in Fig. 3. The measure of the interference is an unknown phase Φ. We vary Φ over its whole range and draw some conclusions: 1) The results of two methods do not match for any angle Φ, showing that there is always a nonperturbative interference caused by the coupled-channel. 2) the specific line shape of the dipion

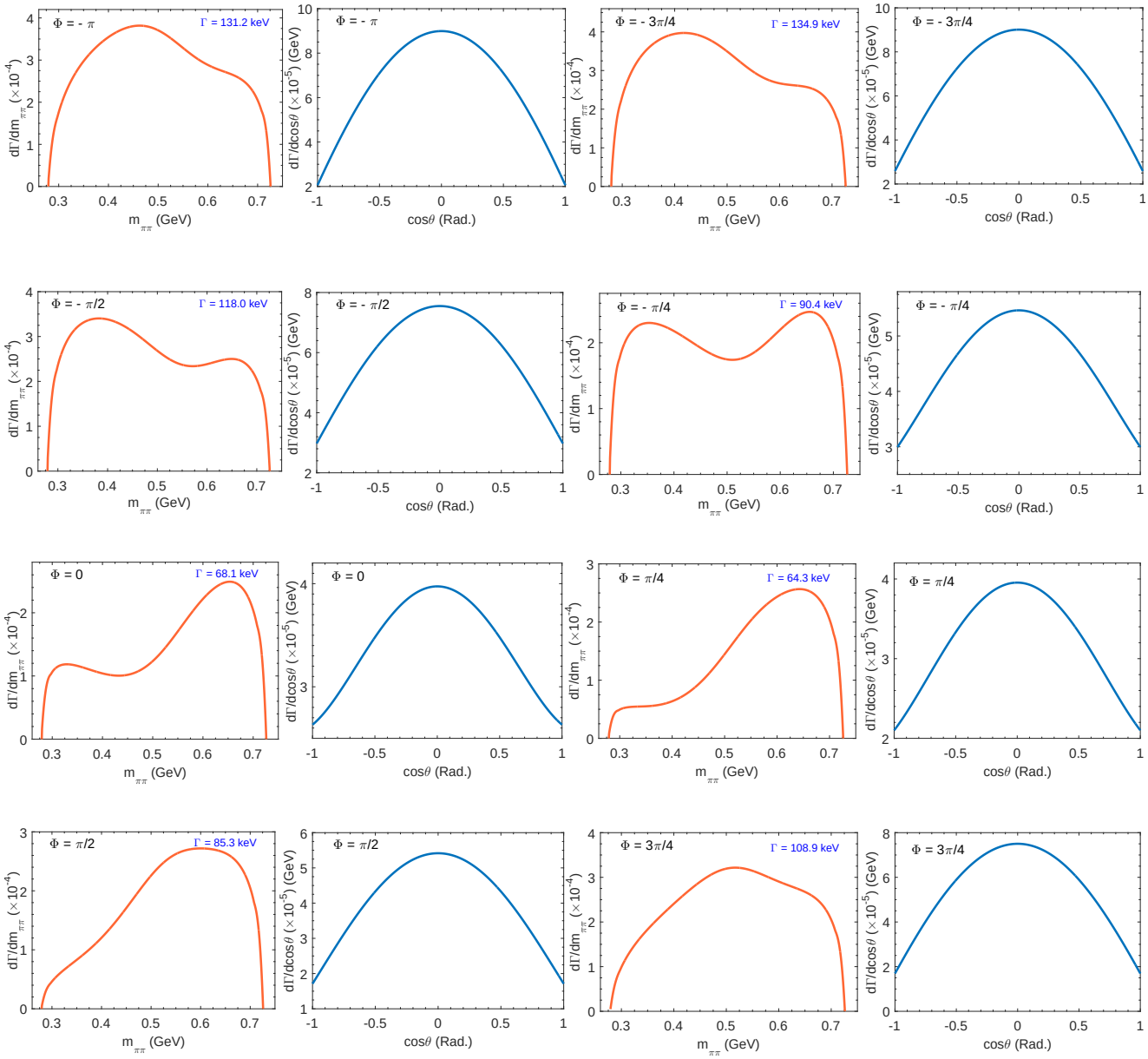

FIG. 6: The $\pi^+\pi^-$ invariant mass distribution $d\Gamma[X(3823) \to J/\psi\pi^+\pi^-]/dm_{\pi^+\pi^-}$ and the angular distribution $d\Gamma[X(3823) \to J/\psi\pi^+\pi^-]/d\cos\theta$ including the coupled-channel effect. Here, typical values of the phase angle Φ are taken, and the corresponding total decay width is listed.

invariant mass changes dramatically with Φ, but the E705 data excludes values between $[-\pi, -\pi/4]$ and $[\pi/4, 3\pi/4]$. 3) For small Φ angles, the decay distribution over the scattering angle θ is mostly in the perpendicular direction in relation with the momentum of the $X(3823)$. 4) Scenarios in Fig. 6 corresponding to Φ between $[0, \pi/4]$ are favored. 5) Favored scenarios correspond to partial decay widths $\Gamma(X(3823) \to J/\psi\pi^+\pi^-)$ between 68.1 and 64.3 keV, values much within the experimental upper limit of 16 MeV.

Motivated by our nonperturbative coupled-channel results, we suggest new experimental studies in channel $X(3823) \to J/\psi\pi^+\pi^-$, which should be analyzed in terms of the $m_{\pi^+\pi^-}$ invariant mass distribution, and in the scattering angle distribution as well. We stress that such an analysis in this golden channel is relevant, not only to establish the expected hadronic decay of $\psi(1^3D_2)$, but will also provide theoretical insight into the contribution of coupled-channel effects in hadronic transitions. Indeed, the present work already shows that the OZI-allowed channel, although it is closed, yet relatively nearby, influences an OZI-suppressed decay, however only experiment will allow us to quantify the strength of this influence and determine the Φ parameter. Nevertheless, we can already conclude that any realistic description of any hadron state should not neglect the nearby OZI-allowed hadronic decay channels. If this is true for the present state, which is not radially excited and is still below any opened channels, it will be even more true for the higher radially excited resonances or for light-quark systems.

Acknowledgments

This project is supported by the National Natural Science Foundation of China under Grant Nos. 11222547, 11175073, 11375240, and 11035006; the Ministry of Education of China (SRFDP under Grant No. 2012021111000); and the Chinese Academy of Sciences under the funding Y104160YQ0 and agreement No. 2015-BH-02. This work is also supported by Fermilab, operated by the Fermi Research Alliance, LLC, U.S. Department of Energy, Contract DE-AC02-07CH11359 (EE).

[1] E. S. Swanson, Phys. Rept. **429**, 243 (2006).
[2] S. L. Zhu, Int. J. Mod. Phys. E **17**, 283 (2008).
[3] N. Brambilla, S. Eidelman, B. K. Heltsley, R. Vogt, G. T. Bodwin, E. Eichten, A. D. Frawley and A. B. Meyer *et al.*, Eur. Phys. J. C **71**, 1534 (2011).
[4] X. Liu, Chin. Sci. Bull. **59**, 3815 (2014).
[5] S. L. Olsen, Front. Phys. **10**, 101401 (2015).
[6] C. Z. Yuan, Front. Phys. **10**, 101401 (2015)
[7] J. Beringer *et al.* [Particle Data Group Collaboration], Chins. Phys. C **38**, 090001 (2014).
[8] S. Godfrey and N. Isgur, Phys. Rev. D **32**, 189 (1985).
[9] E. Eichten, K. Gottfried, T. Kinoshita, K. D. Lane and T. M. Yan, Phys. Rev. D **17**, 3090 (1978) [Erratum-ibid. D **21**, 313 (1980)].
[10] L. Antoniazzi *et al.* [The E705 Collab.], Phys. Rev. D **50**, 4258 (1994).
[11] V. Bhardwaj *et al.* [The Belle Collab.], Phys. Rev. Lett. **111**, no. 3, 032001 (2013).
[12] M. Ablikim *et al.* [The BESIII Collab.] Phys. Rev. Lett. **115**, 011803 (2015).
[13] E. J. Eichten, K. Lane and C. Quigg, Phys. Rev. Lett. **89**, 162002 (2002).
[14] D. Ebert, R. N. Faustov and V. O. Galkin, Phys. Rev. D **67**, 014027 (2003).
[15] P. w. Ko, J. Lee and H. S. Song, Phys. Lett. B **395**, 107 (1997).
[16] C. F. Qiao, F. Yuan and K. T. Chao, Phys. Rev. D **55**, 4001 (1997).
[17] Y. P. Kuang, Front. Phys. China **1**, 19 (2006).
[18] X. Liu, X. Q. Zeng and X. Q. Li, Phys. Rev. D **74**, 074003 (2006).
[19] Y. A. Simonov, Phys. Atom. Nucl. **71**, 1048 (2008).
[20] X. Liu, B. Zhang and X. Q. Li, Phys. Lett. B **675**, 441 (2009).
[21] Y. J. Zhang, G. Li and Q. Zhao, Phys. Rev. Lett. **102**, 172001 (2009).
[22] D. Y. Chen, X. Liu and X. Q. Li, Eur. Phys. J. C **71**, 1808 (2011).
[23] D. Y. Chen, X. Liu and T. Matsuki, Phys. Rev. D **90**, 034019 (2014).
[24] Y. P. Kuang, S. F. Tuan and T. M. Yan, Phys. Rev. D **37**, 1210 (1988).
[25] G. Rupp, E. van Beveren, S. Coito Acta Phys. Polon. Suppl. **8**, 139 (2015).
[26] T. M. Yan, Phys. Rev. D **22**, 1652 (1980).
[27] Y. P. Kuang and T. M. Yan, Phys. Rev. D **24**, 2874 (1981).
[28] W. Buchmuller and S. H. H. Tye, Phys. Rev. Lett. **44**, 850 (1980).
[29] M. B. Voloshin, Phys. Rev. D **91**, 114029 (2015).
[30] D. Y. Chen, X. Liu and S. L. Zhu, Phys. Rev. D **84**, 074016 (2011).
[31] D. Y. Chen, J. He, X. Q. Li and X. Liu, Phys. Rev. D **84**, 074006 (2011).
[32] D. Y. Chen and X. Liu, Phys. Rev. D **84**, 034032 (2011).
[33] C. Meng and K. T. Chao, Phys. Rev. D **75**, 114002 (2007).
[34] M. B. Voloshin and V. I. Zakharov, Phys. Rev. Lett. **45**, 688 (1980).
[35] M. B. Voloshin, Phys. Rev. D **74**, 054022 (2006).
[36] R. Casalbuoni, A. Deandrea, N. Di Bartolomeo, R. Gatto, F. Feruglio and G. Nardulli, Phys. Rept. **281**, 145 (1997).
[37] R. Casalbuoni, A. Deandrea, N. Di Bartolomeo, R. Gatto, F. Feruglio and G. Nardulli, Phys. Lett. B **309**, 163 (1993).
[38] P. Colangelo, F. De Fazio and T. N. Pham, Phys. Rev. D **69**, 054023 (2004).
[39] X. Liu, B. Zhang and S. L. Zhu, Phys. Lett. B **645**, 185 (2007).
[40] D. Y. Chen, X. Liu and T. Matsuki, Phys. Rev. D **88**, no. 3, 036008 (2013).
[41] A. Deandrea, G. Nardulli and A. D. Polosa, Phys. Rev. D **68**, 034002 (2003).
[42] N. N. Achasov and A. A. Kozhevnikov, Phys. Rev. D **49**, 275 (1994).
[43] R. D. Matheus, F. S. Navarra, M. Nielsen and R. Rodrigues da Silva Phys. Lett. B **541**, 265 (2002).
[44] X. Liu, Y. R. Liu, W. Z. Deng and S. L. Zhu, Phys. Rev. D **77**, 094015 (2008).
[45] W. A. Bardeen, E. J. Eichten and C. T. Hill, Phys. Rev. D **68**, 054024 (2003).
[46] T. Komada, S. Ishida and M. Ishida, Phys. Lett. B **508**, 31 (2001).